Fusion of the $^{16}O + ^{76}Ge$ and $^{18}O + ^{74}Ge$ systems and the role of positive Q-value neutron transfers

H. M. Jia, C. J. Lin,* F. Yang, X. X. Xu, H. Q. Zhang, Z. H. Liu, L. Yang, S. T. Zhang, P. F. Bao, and L. J. Sun
China Institute of Atomic Energy, P. O. Box 275(10), Beijing 102413, P. R. China
(Received 26 June 2012; published 22 October 2012)

Fusion excitation functions with high precision have been measured for the $^{16}O + ^{76}Ge$ and $^{18}O + ^{74}Ge$ systems at energies near and below the Coulomb barrier. The barrier distributions have been extracted from the corresponding excitation functions. The coupling effect of the positive Q-value neutron transfer channel in the heavy-ion fusion reaction was examined by a comparison of the two systems. The fusion excitation functions are well reproduced by coupled-channels calculations including the 2^+ and 3^- vibrational states of the targets and the 2^+ rotational state of ^{18}O projectile. No obvious fusion enhancement due to the positive Q-value two-neutron transfer for the $^{18}O + ^{74}Ge$ system is observed as compared with the reference system of $^{16}O + ^{76}Ge$. Analogous systems which are available in the literature are also discussed to realize the role of one- and/or two-neutron transfers with positive Q values in the fusion process.

DOI: 10.1103/PhysRevC.86.044621 PACS number(s): 25.70.Gh, 25.70.Jj, 24.10.Eq

I. INTRODUCTION

The role of neutron transfer in the fusion process is an important topic of current interest. The importance stems from the intuition that neutron transfers occur at a distance beyond the Coulomb barrier and, therefore, may have an obvious influence on the subsequent fusion reaction which occurs inside the barrier. In theory, it has been proposed for more than three decades by Beckerman *et al.* [1] that multiple transfers or exchange processes occur near or at the distance of closet approach may serve as doorway states to fusion. The transfers of nucleon(s) with positive Q values produce an increase in the kinetic energy and favor fusion [2]. Broglia *et al.* [3] claimed that the favorable Q-value transfer channel gives rise to a large enhancement at the sub-barrier fusion cross section. Henning *et al.* [4] noticed a direct correlation between the overall transfer strength and fusion enhancement. Stelson *et al.* [5] thought that a flow of neutrons between the reactants had already started before fusion took place. Based on the idea of the additional kinematic energy increase due to the positive Q-value neutron transfer (PQNT), Zagrebaev [6] proposed a simplified semiclassical model to describe the effects of sequential neutron transfers in an approximate way, which can explain the sub-barrier fusion enhancement. Experimentally, some signatures have shown that couplings to the PQNT enhance the fusion cross sections, especially at sub-barrier energies. For example, systematic research for the reaction systems of $^{28}Si + ^{94}Zr$ [7], $^{32}S + ^{96}Zr$, ^{100}Mo, ^{110}Pd [8–10], and $^{40}Ca + ^{48}Ca$, ^{96}Zr, $^{124,132}Sn$ [11–15] has confirmed the fusion enhancement due to the PQNT channels by comparison with their reference systems.

However, the relationship between fusion and neutron transfer is actually not clear yet. Theoretically, other mechanisms can also explain the experimental results without including the PQNT effects explicitly. For example, for the $^{40}Ca + ^{96}Zr$ system, both the enhancement of fusion cross sections and the shape of barrier distribution (BD) can be well reproduced by a semiclassical model, mainly considering the coupling of the strong octupole vibrational state of ^{96}Zr [16]. Besides the coupled-channels (CC) method mentioned above, other theories such as the quantum molecular dynamics model [17] as well as the time-dependent Hartree-Fock method [18] likewise reproduced the fusion excitation functions successfully without considering the details of couplings. Experimentally, there exist some negative observations. In the systems of $^{18}O + ^{92}Mo, ^{118}Sn$ [19,20], $^{36}S + ^{58}Ni$ [21], and $^{58}Ni + ^{100}Mo$, ^{124}Sn [22–24], the fusion cross sections do not show additional enhancement at sub-barrier energies due to the PQNT channels. For $^{36}S + ^{58}Ni$ and $^{18}O + ^{118}Sn$, it was ascribed to kinematic mismatches for the transfer reactions [20,21]. Recently, Kohley *et al.* [25] observed that fusion of the neutron-rich $^{132}Sn + ^{58}Ni$ system, with more PQNT channels, does not cause any enhancement in fusion cross sections down to the ∼5-mb level by means of a systematic comparison to its references. Later, Sargsyan *et al.* [26] tentatively presented a theoretical explanation that the neutron transfers influence the sub-barrier capture through the changes of the deformations of the colliding nuclei.

Until now, such a coupling is still difficult to be taken into account precisely in CC calculations [27]. It is strongly desired to develop a consistent microscopic approach to clarify unambiguously the role of neutron transfer in the fusion process, especially the PQNT effect on heavy-ion fusion at sub-barrier energy. Extended experimental research, particularly on the simple cases of one-neutron ($1n$) and two-neutron ($2n$) transfers with positive Q values, will push the development of theory.

To avoid added ambiguities, one may propose to measure the fusion cross sections for the systems of which the same compound nucleus (CN) is formed, such as the $^{16}O + ^{76}Ge$ and $^{18}O + ^{74}Ge$ systems selected in this work. The corresponding excitation-energy levels and deformation parameters are quite similar for the two targets. The deformation effect of ^{18}O is minor [28] and ^{16}O is spherical. The main difference in the two systems comes from the transfer reaction. The $^{18}O + ^{74}Ge$ system possesses a positive Q-value $2n$ transfer channel, while the $^{16}O + ^{76}Ge$ system has no such reaction channel. The latter

*Corresponding author: cjlin@ciae.ac.cn

can be used as a reference system to explore the PQNT effect on the former, where the $2n$ transfer is a simpler case which can be included in the CC calculations [27] as a pair transfer.

In the present paper, we report the measurements of fusion excitation functions for the $^{16}O + ^{76}Ge$ and $^{18}O + ^{74}Ge$ systems. Our research will focus on the role of positive Q-value $2n$ transfer on sub-barrier fusion. This paper is organized as follows. Section II presents the experimental setup and details of the measurements. Results of the analysis of experimental data and the CC calculations are described in Sec. III. Discussions on the role of positive Q-value $1n$ and $2n$ transfers are given in Sec. IV. Finally, Sec. V gives a brief summary.

II. EXPERIMENTAL PROCEDURES

The experiment was performed at the HI-13 tandem accelerator of the China Institute of Atomic Energy (CIAE), Beijing, China. Collimated $^{16,18}O$ ($q = 5^+$) beams with an intensity of 20–30 pnA were used to bombard the $^{76,74}Ge$ targets. The beam energies were varied in the range 38–61 MeV and changed only downward in energy in order to reduce the magnetic hysteresis. The 3-mm diameter ^{74}Ge (99.7% enriched) and 5-mm diameter ^{76}Ge (99.9% enriched) targets were 120 $\mu g/cm^2$ thick evaporated onto 30-$\mu g/cm^2$ carbon foil backing and 50 $\mu g/cm^2$ thick evaporated onto 20-$\mu g/cm^2$ carbon foil backing, respectively. Four silicon (Si) detectors placed symmetrically at $\theta_{lab} = \pm 20^\circ$ (right-left and up-down) with respect to the beam direction were used to monitor the Rutherford scatterings and to provide a normalization of the fusion cross section.

Fusion evaporation residues (ERs) mainly concentrated within a few degrees of the incident beam direction were separated from the beamlike particles (BLPs) by using an electrostatic deflector setup [29]. It consists of two pairs of electrodes followed by time-of-flight (TOF) versus E detector telescopes with two microchannel plate (MCP) detectors and a 48×48 mm^2 quadrant Si detector. Distances of MCP1-MCP2 and MCP2-Si are 41.0 and 22.7 cm, respectively. TOF1-E (TOF1: MCP1-Si) and TOF2-E (TOF2: MCP2-Si) spectra are very useful to reduce the spurious backgrounds from the random coincidences between the Si and one of the MCPs, especially for the measurements of low fusion cross sections at sub-barrier energies and for such asymmetric systems studied in this work. Figure 1 shows a typical TOF1 versus E spectrum for the $^{18}O + ^{74}Ge$ system at an energy near the Coulomb barrier, where the BLPs and ERs can be separated clearly.

The particles from the target were selected before entering the electric fields by an entrance collimator of 2.5 mm in diameter, corresponding to an opening angle $\theta_{lab} = \pm 0.38^\circ$. A 10-$\mu g/cm^2$-thick carbon foil 19 cm downstream of the target was used to reset the atomic charge state distribution by an internal conversion process on the ion path.

The ERs angular distributions were measured in the range $\theta_{lab} = -5^\circ$ to $+13^\circ$ with step $\Delta\theta_{lab} = 1^\circ$ for $^{16}O + ^{76}Ge$ at $E_{lab} = 44.38$ MeV and $^{18}O + ^{74}Ge$ at $E_{lab} = 45.40$ and 40.39 MeV, respectively. Their typical shapes do not change appreciably with the beam energy and give an overall width of

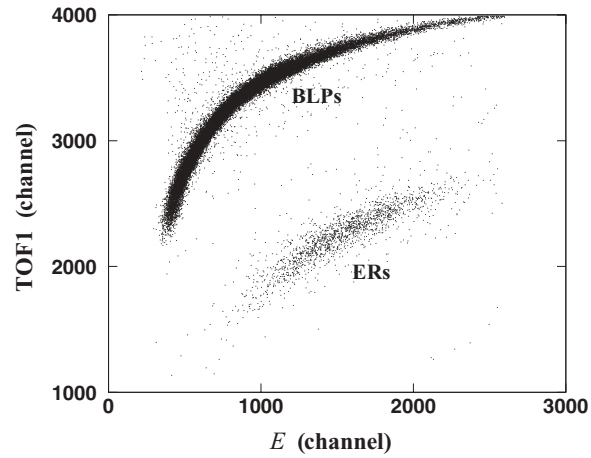

FIG. 1. Two-dimensional plot TOF1-E taken at $E_{lab} = 42.89$ MeV and $\theta_{lab} = 3^\circ$ for $^{18}O + ^{74}Ge$. A group of BLPs and ERs are indicated.

4.3° symmetrical about $\theta_{lab} = 0^\circ$, as shown in Fig. 2. The ERs angular distributions were fitted by a single Gaussian function resulting from the dominant neutron and/or proton evaporation from the CN, which is consistent with the calculation of the code PACE2 [30]. The fusion cross sections were obtained by integration of the angular distribution and normalized by the Rutherford scatterings counted by the Si monitors.

For most energies, the differential cross sections have been measured only at $\theta_{lab} = 3^\circ$. The total ERs cross sections were deduced from the ratio of the value measured at $\theta_{lab} = 3^\circ$ to the Gaussian fitted ERs angular distribution and normalized by the area of the whole distribution. Meanwhile, corrections were made for the solid angles and transmission efficiencies. Since fission of the CN can be neglected for both systems, the measured ERs cross sections were regarded as complete fusion cross sections σ_{Fus}.

The transmission efficiencies and the relevant voltages used to deflect the ERs were calibrated with ^{79}Br and ^{127}I beams

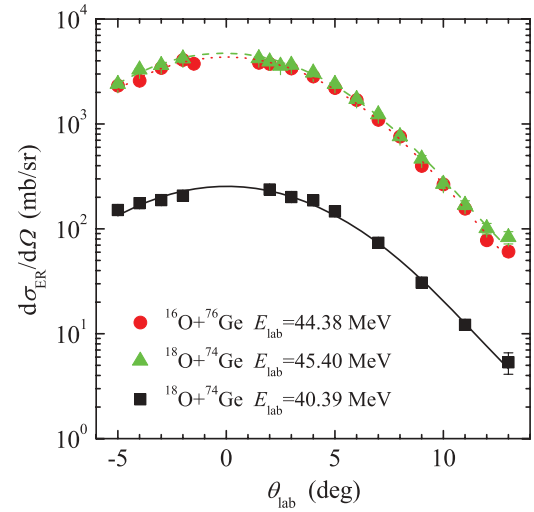

FIG. 2. (Color online) The angular distributions of ERs of $^{16}O + ^{76}Ge$ and $^{18}O + ^{74}Ge$. The lines are the single Gaussian fits used to obtain the total fusion cross sections.

TABLE I. Experimental fusion cross sections for $^{16}O + ^{76}Ge$; quoted errors are only statistical uncertainties.

$E_{c.m.}$ (MeV)	σ_{Fus} (mb)	$E_{c.m.}$ (MeV)	σ_{Fus} (mb)
50.1	885.1 ± 7.9	37.2	167.4 ± 2.2
48.1	773.6 ± 7.2	36.7	144.7 ± 2.1
46.1	682.7 ± 6.4	36.2	113.8 ± 1.6
44.1	579.1 ± 5.1	35.7	90.0 ± 1.5
43.1	543.0 ± 5.2	35.2	66.4 ± 1.2
42.1	471.4 ± 4.6	34.7	47.2 ± 0.8
41.1	414.1 ± 4.2	34.2	30.8 ± 0.6
40.1	343.2 ± 3.4	33.7	20.0 ± 0.5
39.6	321.9 ± 3.2	33.2	10.5 ± 0.3
39.1	291.8 ± 2.9	32.7	6.31 ± 0.22
38.6	257.4 ± 2.6	32.2	1.90 ± 0.11
38.1	226.6 ± 2.6	31.7	0.92 ± 0.07
37.7	190.9 ± 2.3	31.2	0.37 ± 0.03

scattered by a ^{208}Pb target at the corresponding energies to the ERs at 13°. It was found that the defocusing effect of the deflection voltage reduces the transmission to 0.29 ± 0.03. Altogether a systematic error of 15% is estimated considering additional systematic errors, which come from the uncertainties of geometrical solid angle, the angular distribution integrations, and the transmission measurements.

III. EXPERIMENTAL RESULTS

The measured fusion cross sections are listed in Tables I and II and the corresponding excitation functions are shown in Figs. 3 and 4 for $^{16}O + ^{76}Ge$ and $^{18}O + ^{74}Ge$, respectively, where the energy scales have been corrected for the carbon backings (faced to beams) and the target thicknesses. The highest energies are at 40% above the Coulomb barriers. The statistical uncertainties are of the order of 1% for the higher and intermediate energy data and increasing to 8% for the lowest ones.

The data were analyzed using the code CCFULL [27] with all order couplings. The standard Akyüz-Winther (AW) potentials [31] were utilized. The potential parameters,

TABLE II. Same as Table I but for $^{18}O + ^{74}Ge$.

$E_{c.m.}$ (MeV)	σ_{Fus} (mb)	$E_{c.m.}$ (MeV)	σ_{Fus} (mb)
49.0	847.9 ± 7.9	36.0	136.5 ± 1.2
46.9	731.6 ± 7.6	35.5	99.4 ± 0.9
46.0	686.5 ± 7.4	35.0	82.6 ± 0.8
44.0	593.4 ± 4.8	34.5	63.1 ± 0.6
43.0	545.6 ± 4.4	34.0	46.9 ± 0.4
41.9	497.9 ± 3.7	33.5	31.5 ± 0.3
40.9	409.9 ± 3.3	33.0	16.7 ± 0.2
39.9	371.3 ± 2.3	32.5	10.0 ± 0.1
38.9	292.5 ± 2.7	32.0	4.56 ± 0.08
38.0	254.8 ± 1.8	31.5	1.84 ± 0.05
37.5	211.9 ± 2.0	31.0	0.89 ± 0.03
37.0	190.1 ± 1.6	30.5	0.25 ± 0.01
36.5	156.7 ± 1.3	30.2	0.14 ± 0.01

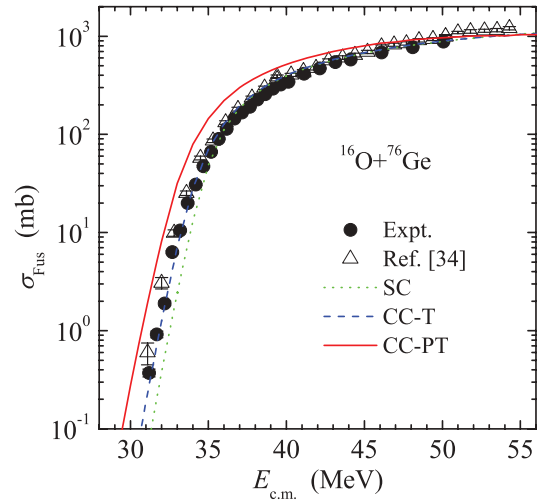

FIG. 3. (Color online) Fusion excitation function for the $^{16}O + ^{76}Ge$ system. The solid circles are our experimental data. The dotted, dashed, and solid lines represent the SC calculation, the CC calculations including the target excitation only and including both the projectile and target excitations, respectively. The data from Ref. [34] are also shown as open triangles.

together with the deduced barrier parameters, are reported in Table III. These potential parameters have been used without any attempt to vary them to fit the above-barrier data. The relevant information on the low-lying states of $^{16,18}O$ and $^{74,76}Ge$ included in the CC calculations were calculated from the measured transition probabilities $B(E2\uparrow)$ [32] and $B(E3\uparrow)$ [33] using the expression

$$\beta_\lambda = \frac{4\pi}{3ZR^\lambda}\sqrt{\frac{B(E\lambda\uparrow)}{e^2}},$$

where the nuclear radius $R = r_0 A^{1/3}$ and $r_0 = 1.20$ fm. The same Coulomb and nuclear deformations were considered in the calculations. These parameters are listed in Table IV for reference.

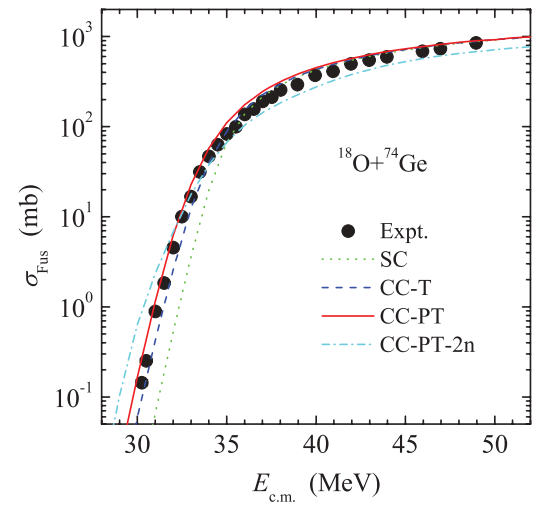

FIG. 4. (Color online) Same as Fig. 3 but for the $^{18}O + ^{74}Ge$ system. The dash-dotted line represents the CC calculation including additional coupling of $2n$-pair transfer.

TABLE III. Parameters of the AW potential used in our CC calculations together with barrier heights, radii, and curvatures resulting from the potentials.

System	V_0 (MeV)	r_0 (fm)	a (fm)	V_B (MeV)	R_B (fm)	$\hbar\omega$ (MeV)
$^{16}O+^{76}Ge$	56.48	1.173	0.640	34.77	9.89	3.80
$^{18}O+^{74}Ge$	56.46	1.174	0.643	34.45	9.98	3.59

For $^{16}O+^{76}Ge$, the low-lying vibrational 2^+ and 3^- one-phonon states of the target, the same ones used in Ref. [34], as well as their mutual excitations were included in the calculations. The single-channel (SC) and CC calculation including target excitation only (CC-T) are shown as dotted and dashed lines in Fig. 3, respectively. It shows that the CC calculation including the target vibrational states reproduces the excitation function rather well within the given uncertainties of the experimental cross sections. The higher excitation energy of the 3^- one-phonon state of ^{16}O only produces an adiabatic potential renormalization without affecting the structure in the BD [35], and, consequently, including this state (CC-PT) induces an overestimate for the experimental data.

^{74}Ge is a good vibrator: Its lowest 2^+ state lies at 596 keV only and is connected to the ground state by an $E2$ transition of 33 W.u.. A triplet of state $(4^+,2^+,0^+)$ is known at 1.2–1.5 MeV. One can consider the surface vibration up to the two-phonon level. In the case of $^{18}O+^{74}Ge$, the calculation of SC (dotted line) and the CC calculations including the target 2^+ two-phonon and 3^- one-phonon vibrational states alone (dashed line) and also including the 2^+ state of ^{18}O (solid line) are shown in Fig. 4, respectively. The CC-T calculation somewhat underestimates the excitation function at sub-barrier energies, while the CC-PT calculation fits the experimental data much better. In order to check the effects of neutron transfer, the CC calculation was also performed by including the additional $2n$-pair transfer channel with a positive Q value of 3.75 MeV and the nominal coupling strength of 0.7 MeV. Result is illustrated as the dash-dotted line (CC-PT-2n) in Fig. 4 for a qualitative comparison. One can see that the trend deviates distinctly from the fusion data at the whole energy region. It indicates that the neutron transfer can be negligible for this system at the measured energy range.

The reduced fusion excitation functions for the two systems are shown in Fig. 5(a) for comparison. It may be seen that no significant differences are observed in the fusion excitation functions of two systems at least down to the 0.1-mb level. This provides further experimental evidence that, in some cases, the coupling effects of the PQNT channel on the fusion process at the measured energy range are very limited.

TABLE IV. Excitation energies E_x, spins and parities λ^π, and deformation parameters β_λ for $^{16,18}O$ and $^{74,76}Ge$.

Nucleus	E_x (MeV)	λ^π	$B(E\lambda\uparrow)$ (e^2 b$^{2\lambda}$)	β_λ
^{16}O	6.13	3^-	0.00141	0.71
^{18}O	1.98	2^+	0.00451	0.36
^{74}Ge	0.60	2^+	0.320	0.29
	2.54	3^-	0.024	0.16
^{76}Ge	0.56	2^+	0.280	0.27
	2.69	3^-	0.020	0.14

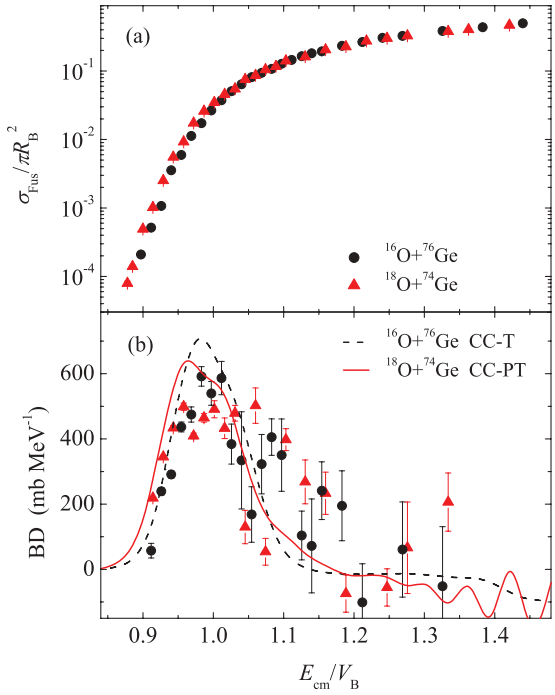

FIG. 5. (Color online) (a) Plot of the reduced fusion excitation functions on a reduced energy scale for the two systems. (b) Barrier distributions extracted from fusion excitation functions are compared with the CC results.

The fusion BDs for the two systems were deduced from the fusion cross sections as the curvature of $E_{c.m.}\sigma_{Fus}$ [36]. A three-point formula with a variable energy step was used for the numerical evaluation of the second derivatives with our data; $\Delta E_{c.m.} = 2.0$ MeV for higher energies and $\Delta E_{c.m.} = 1.5$ MeV for the energies below the barrier. Little information was lost because the energy steps nearly match the half of the curvatures of the Coulomb barrier (see Table III). The corresponding BDs are shown in Fig. 5(b). No normalizations have been done for the BDs due to the large oscillations at higher energies. Both experimental fusion BDs show a main peak centered around the barrier with a width of ~4 MeV. The corresponding CC calculations for $^{16}O+^{76}Ge$ and $^{18}O+^{74}Ge$ are shown by dashed and full lines, respectively. The CC results qualitatively reproduce the experimental BDs.

IV. DISCUSSION

In this work, the $^{18}O+^{74}Ge$ system does not show additional fusion enhancement at the sub-barrier energy region compared with the $^{16}O+^{76}Ge$ system. Despite the positive Q_{-2n} (+3.75-MeV) neutron transfer channel for the former, the fusion behavior of the two systems is almost the same. The CC calculations can reproduce the experimental fusion excitation functions rather well and reproduce the BDs qualitatively when the couplings to the low-lying excitation

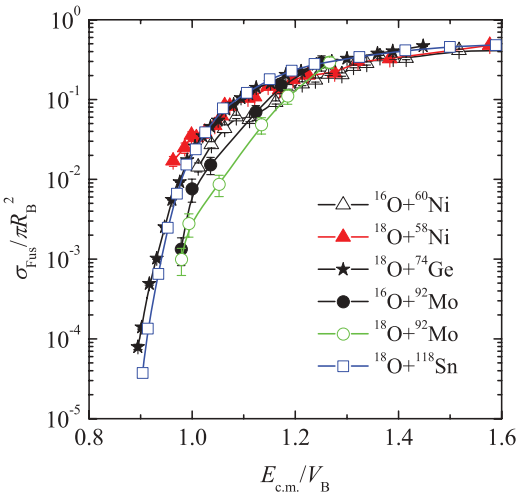

FIG. 6. (Color online) Reduced fusion excitation functions for some typical systems with positive Q-value $2n$ transfers.

states are included only. Whereas the additional coupling of the PQNT channel destroys the reliability of CC calculation for the $^{18}O + ^{74}Ge$ system. No effect of PQNT has been found in this system. The question is whether other systems also behave like that. To investigate more systems may be helpful to answer this question. As mentioned in Sec. I, the effects of multineutron transfers with positive Q values are inconsistent in the fusion reactions, even for some neighbor systems like $^{40}Ca + ^{132}Sn$ and $^{58}Ni + ^{132}Sn$. For the sake of simplicity, in the following we select the systems which have $1n$ and/or $2n$ transfers with positive Q values and the fusion data are available in literature.

For the $1n$ transfer cases, so far the fusion enhancement related to transfer channel was observed only in the $^{17}O + ^{144}Sm$ ($Q_{-1n} = +2.61$ MeV) system with comparison of the reference system of $^{16}O + ^{144}Sm$ [37]. While for other systems, such as $^{17}O + ^{117,124}Sn$ ($Q_{-1n} = +5.18$ MeV and $+1.59$ MeV, respectively), no signatures show the fusion enhancements by comparison with the $^{16}O + ^{117,124}Sn$ systems [20].

For the $2n$ cases, the situation becomes a little bit complicated. Some typical systems are selected and discussed here. The reduced fusion excitation functions are illustrated in Fig. 6 and the relevant Q values are listed in Table V for a systematic comparison. The fusion cross section σ_{Fus} and $E_{c.m.}$ was scaled, by the geometrical cross section $\pi R_B^2 = 10\pi(1.20A_P^{1/3} + 1.06A_T^{1/3})^2$ and the Coulomb barrier $V_B = 0.85247z + 0.001361z^2 - 0.00000223z^3$ MeV [38], to factor out the size and Coulomb barrier differences of the various systems. Where $z = Z_P Z_T/(A_P^{1/3} + A_T^{1/3})$ is the Coulomb parameter, $Z_P(Z_T)$ and $A_P(A_T)$ are the charge and mass of the projectile (target).

TABLE V. Q values from ground-state to ground-state transfers.

System	Q_{1n} (MeV)	Q_{2n} (MeV)
$^{18}O + ^{24}Mg$	−0.71	+6.24
$^{18}O + ^{50}Cr$	+0.84	+9.11
$^{16}O + ^{60}Ni$	−7.24	−8.20
$^{18}O + ^{58}Ni$	+0.96	+8.20
$^{18}O + ^{74}Ge$	−1.54	+3.75
$^{16}O + ^{92}Mo$	−8.53	−10.6
$^{18}O + ^{92}Mo$	+0.03	+5.56
$^{18}O + ^{118}Sn$	−1.56	+3.41
$^{40}Ca + ^{48}Ca$	−1.58	+2.62

For the $^{18}O + ^{58}Ni$ system, fusion enhancement undoubtedly exits although the cross sections were measured near the barrier [39]. Later the BD extracted from the backward quasielastic scattering [40] also supports this point. Borges *et al.* [39] thought that the collective $2n$-pair transfer mode plays an important role. Such enhancement can be explained well by the zero-point pairing fluctuations model (pairing vibrations related to two-neutron transfer channel). The fusion behavior of $^{18}O + ^{74}Ge$ differs markedly from $^{18}O + ^{58}Ni$. For $^{74}Ge(^{18}O,^{16}O)^{76}Ge$, the experiment performed by Bond *et al.* [41] showed that the transfer mainly populates the ground state at 27° with a beam energy of 75 MeV. It denotes that the $2n$ stripping channel is kinematically matched and neutron transfer should enhance the subsequent fusion at sub-barrier energies, as expected from ground-state to ground-state transfer at the sub-barrier region [42]. However, our results do not show such an effect by the comparison of the experimental data with CC calculations. In addition, fusion of $^{18}O + ^{92}Mo$ [19] and $^{18}O + ^{118}Sn$ [20] does not yet show the enhancement as compared with their reference systems. As is demonstrated above, the strong correlation between sub-barrier fusion enhancement and the possession of PQNT observed in $^{18}O + ^{58}Ni$ clearly stands out from $^{18}O + ^{74}Ge$, ^{92}Mo, ^{118}Sn.

It is known that transfer couplings also depend on the states and Q values populated by transferred nucleons and transfer form factors. For ^{18}O induced reaction, the Q value of $2n$ stripping channel is usually positive. It is advantageous to use ^{18}O as projectile to investigate the influence of the $2n$ transfer channel on fusion. However, the relevant fusion data with high accuracy are rather scarce up to now. In order to research the dependence of the fusion on targets at sub-barrier energies, it will be helpful to select the ^{18}O induced reactions with lower $Z_P Z_T$ and higher Q_{-2n}/V_B values. For example, the Q_{-2n}/V_B values for the systems $^{18}O + ^{24}Mg$, ^{50}Cr, ^{58}Ni are $6.24/15.27 = 0.41$, $9.11/27.16 = 0.34$, and $8.20/30.95 = 0.26$, respectively. To measure the fusion excitation functions for these systems with high accuracy may help us to clarify the relevant dynamic mechanisms. On the other hand, direct measurements of the $2n$ transfers are also meaningful for correlating the two aspects of fusion and transfer and constraining the transfer coupling strengths.

Due to the spherical properties, which should reduce deformation effect on fusion, and the positive Q-value of the $2n$ transfer channel, the system $^{40}Ca + ^{48}Ca$ attracts much attention [11,12]. It was pointed out in Ref. [43] that a strong pair-transfer channel with a positive Q value was necessary to be taken into account in the CC calculations. The elastic scattering data near the barrier also show such a strong coupling [44]. Zagrebaev [6] interpreted the fusion data by assuming the sequential neutron transfer, similarly to Stelson's neutron flow picture. Very recently, Keser *et al.* [18] reproduced the data by using a DC-TDHF method, which shows that the neutron transfer only starts mainly inside the

Coulomb barrier; this means PQNT cannot enhance the initial kinetic energy but only alters the nuclear potential inside the barrier. This point of view differs substantially from the prevailing argument that neutron transfer starts at a larger separation. It shows that the reaction mechanisms of transfer couplings to fusion process are quite complicated beyond the considerations of up-to-date models. It is a great challenge to unveil the *hidden* aspect of the reaction dynamics and to understand the role transfer plays in fusion in both experiment and theory.

V. SUMMARY

In summary, fusion cross sections have been measured for the $^{16}O + ^{76}Ge$ and $^{18}O + ^{74}Ge$ systems at energies near and below the barrier. The BDs were extracted from the second derivative of the excitation functions. The fusion behavior of the two systems shows remarkable similarities and can be reproduced well by the CC calculations with the low-lying inelastic states being taken into account for the two systems. This is beyond the expectation for $^{18}O + ^{74}Ge$ in the case of a positive Q_{-2n} neutron transfer channel.

The effect of neutron transfer on fusion is still an open question. The controversial PQNT effect on fusion observed in the fusion reactions has presented a challenge for the theoretical understanding of the reaction mechanism. It is highly desired to search for the origin responsible for these inconsistencies of fusion in correlation with PQNT channels and to improve the CC theory or other models.

ACKNOWLEDGMENTS

This work has been supported by the 973 Program of China (Grant No. 2013CB834404) and the National Natural Science Foundation of China (Grants No. 11005154, No. 10975192, No. 11075216, No. 10727505, and No. 11005156).

[1] M. Beckerman *et al.*, Phys. Rev. Lett. **45**, 1472 (1980).
[2] M. Beckerman, M. K. Salomaa, J. Wiggins, and R. Rohe, Phys. Rev. C **28**, 1963 (1983).
[3] R. A. Broglia, C. H. Dasso, S. Landowne, and A. Winther, Phys. Rev. C **27**, 2433 (1983).
[4] W. Henning, F. L. H. Wolfs, J. P. Schiffer, and K. E. Rehm, Phys. Rev. Lett. **58**, 318 (1987).
[5] P. H. Stelson, H. J. Kim, M. Beckerman, D. Shapira, and R. L. Robinson, Phys. Rev. C **41**, 1584 (1990).
[6] V. I. Zagrebaev, Phys. Rev. C **67**, 061601(R) (2003).
[7] S. Kalkal *et al.*, Phys. Rev. C **81**, 044610 (2010).
[8] H. Q. Zhang *et al.*, Phys. Rev. C **82**, 054609 (2010).
[9] H.-J. Hennrich *et al.*, Phys. Lett. B **258**, 275 (1991).
[10] A. M. Stefanini *et al.*, Phys. Rev. C **52**, R1727 (1995).
[11] M. Trotta, A. M. Stefanini, L. Corradi, A. Gadea, F. Scarlassara, S. Beghini, and G. Montagnoli, Phys. Rev. C **65**, 011601(R) (2001).
[12] H. A. Aljuwair *et al.*, Phys. Rev. C **30**, 1223 (1984).
[13] H. Timmers *et al.*, Nucl. Phys. A **633**, 421 (1998).
[14] F. Scarlassara *et al.*, Nucl. Phys. A **672**, 99 (2000).
[15] J. J. Kolata *et al.*, Phys. Rev. C **85**, 054603 (2012).
[16] G. Pollarolo and A. Winther, Phys. Rev. C **62**, 054611 (2000).
[17] Ning Wang, Zhuxia Li, Xizhen Wu, Junlong Tian, Yingxun Zhang, and Min Liu, Phys. Rev. C **69**, 034608 (2004).
[18] R. Keser, A. S. Umar, and V. E. Oberacker, Phys. Rev. C **85**, 044606 (2012).
[19] M. Benjelloun, W. Galster, and J. Vervier, Nucl. Phys. A **560**, 715 (1993).
[20] P. Jacobs, Z. Fraenkel, G. Mamane, and I. Tserruya, Phys. Lett. B **175**, 271 (1986).
[21] A. M. Stefanini *et al.*, Nucl. Phys. **456**, 509 (1986).
[22] F. Scarlassara *et al.*, EPJ Web Conf. **17**, 05002 (2011).
[23] F. L. H. Wolfs, Phys. Rev. C **36**, 1379 (1987).
[24] K. T. Lesko *et al.*, Phys. Rev. C **34**, 2155 (1986).
[25] Z. Kohley *et al.*, Phys. Rev. Lett. **107**, 202701 (2011).
[26] V. V. Sargsyan, G. G. Adamian, N. V. Antonenko, W. Scheid, and H. Q. Zhang, Phys. Rev. C **85**, 024616 (2012).
[27] K. Hagino, N. Rowley, and A. T. Kruppa, Comput. Phys. Commun. **123**, 143 (1999).
[28] E. Vulgaris, L. Grodzins, S. G. Steadman, and R. Ledoux, Phys. Rev. C **33**, 2017 (1986).
[29] H. Q. Zhang *et al.*, Chin. Phys. C **34**, 1628 (2010).
[30] A. Gavron, Phys. Rev. C **21**, 230 (1980).
[31] Ö. Akyüz and A. Winther, in *Nuclear Structure and Heavy-Ion Reactions*, Proceedings of the International School of Physics "Enrico Fermi,"Course LXXVII, Varenna, edited by R. A. Broglia *et al.* (North-Holland, Amsterdam, 1981).
[32] S. Raman, C. W. Nestor, Jr., and P. Tikkanen, At. Data Nucl. Data Tables **78**, 1 (2001).
[33] T. Kibédi and R. H. Spear, At. Data Nucl. Data Tables **80**, 35 (2002).
[34] E. F. Aguilera, J. J. Kolata, and R. J. Tighe, Phys. Rev. C **52**, 3103 (1995).
[35] K. Hagino, N. Takigawa, M. Dasgupta, D. J. Hinde, and J. R. Leigh, Phys. Rev. Lett. **79**, 2014 (1997).
[36] N. Rowley, G. R. Stachler, and P. H. Stelson, Phys. Lett. B **254**, 25 (1991).
[37] C. R. Morton *et al.*, Phys. Rev. Lett. **72**, 4074 (1994).
[38] W. J. Świątecki, K. Siwek-Wilczyńska, and J. Wilczyński, Phys. Rev. C **71**, 014602 (2005).
[39] A. M. Borges, C. P. daSilva, D. Pereira, L. C. Chamon, E. S. Rossi, and C. E. Aguiar, Phys. Rev. C **46**, 2360 (1992).
[40] R. F. Simões *et al.*, Phys. Lett. B **527**, 187 (2002).
[41] P. D. Bond, H. J. Korner, M.-C. Lemaire, D. J. Pisano, and C. E. Thorn, Phys. Rev. C **16**, 177 (1977).
[42] Sunil Kalkal *et al.*, Phys. Rev. C **83**, 054607 (2011).
[43] H. Esbensen, S. H. Fricke, and S. Landowne, Phys. Rev. C **40**, 2046 (1989).
[44] R. J. Tighe, J. J. Kolata, S. Dixit, G. B. Liu, R. J. Vojtech, J. F. Liang, and J. C. Mahon, Phys. Rev. C **42**, R1200 (1990).